

A Dual-Path Architecture for Scaling Compute and Capacity in LLMs

Markus Frey^{1,2,3}, Behzad Shomali^{1,3}, Joachim Koehler^{1,2}, Mehdi Ali^{1,2}

Lamarr Institute¹, Fraunhofer IAIS², University of Bonn³

markus.frey@iais.fraunhofer.de

Abstract

Looped transformers apply a shared block multiple times and have emerged as a parameter-efficient route to scaling compute in language models. However, at fixed FLOPs a looped model has strictly less capacity than a baseline transformer. We propose a novel *dual-path block* that can flexibly scale *compute*, the number of sequential operations applied to a hidden state, and *capacity*, the parameters available at a single step. For this we expose both axes as parallel pathways within a single layer: a *deep* sublayer re-applied K times with shared parameters, and a *wide* sublayer with an enlarged feed-forward network applied once. Independent per-token gates combine both axes and allow detailed per-token routing analyses. We show that across two FLOP budgets, our dual-path model surpasses iso-FLOP matched models on language modeling and downstream evaluations, while using *fewer* parameters than the baseline at matched FLOPs. The learned gates are directly interpretable and show systematic per-token allocation with function words and lexical content trend wide, while punctuation, symbols, and arithmetic tokens trend deep.

1 Introduction

Looped (or recursive) transformers re-apply a shared block K times, trading parameter count for sequential compute (Dehghani et al., 2019; Geiping et al., 2025; Saunshi et al., 2025; Zhu et al., 2025). The appeal is parameter efficiency: L layers looped K times reach the effective depth of KL unshared layers at $1/K$ the parameters, and recent work shows this is enough to recover much of the reasoning performance of a deeper unshared stack (Saunshi et al., 2025; Zhu et al., 2025). However, at fixed FLOPs, a looped model has strictly less capacity than an unshared stack of comparable compute, and the gap shows up empirically on tasks that depend on stored knowledge (Frey et al., 2026; Zhu et al., 2025).

Looping and width scaling therefore sit on two qualitatively different axes of a transformer layer. Looped models use *compute* to increase the number of sequential operations applied to a hidden state, while width-scaled models increase *capacity*, the parameters available at a single step. Standard architectures conflate the two, with every token paying the same cost on both. A looped model puts its whole per-layer feed-forward network (FFN) budget on compute and a width-scaled FFN puts it all on capacity. Neither lets a token that needs more sequential refinement get it without also paying for capacity it does not need, or the other way around.

Recent work relaxes this one axis at a time. Mixture-of-Experts (Shazeer et al., 2017; Fedus et al., 2022) routes tokens to a subset of similar experts, scaling capacity sub-linearly in compute. Mixture-of-Depths (Raposo et al., 2024) routes tokens to skip or apply a layer, varying effective depth per position. Mixture-of-Recursions (Bae et al., 2025) varies the number of loop iterations per token, and adaptive halting mechanisms in looped models do the same via learned stopping (Graves, 2016; Banino et al., 2021; Frey et al., 2026). Each of these routes along a single axis, i.e. which experts, how many loop iterations, or whether to apply a layer at all.

We propose a transformer layer that exposes the two axes separately within itself. Each *dual-path block* contains two parallel sublayers: a *deep* sublayer applied K times with shared parameters (a loop, as above), and a *wide* sublayer with an enlarged feed-forward dimension applied once. A learned per-token gate combines them. We train the dual-path block across different wide and deep ratios (α) and the iso-FLOP controls for each axis separately. We show that:

- At both FLOP budgets, the best dual-path configuration beats both single-axis controls on aggregate language-modelling, commonsense,

and math evaluations *while using fewer parameters than the width-scaled control*.

- The learned gate that mixes the compute and capacity path does not collapse. Its allocation depends systematically on layer index, part-of-speech, and task: function words and lexical content (verbs, adjectives) trend wide, while punctuation, symbols, and arithmetic tokens trend deep.

2 Related Work

Looped and recursive transformers. Re-applying a shared block across depth has been studied as a parameter-efficient route to scaling transformers since the release of Universal Transformers (Dehghani et al., 2019). The idea has been revived recently in language modelling: looped decoders scale test-time compute by re-applying a shared block (Geiping et al., 2025; Saunshi et al., 2025; Zhu et al., 2025; Jeddi et al., 2026) which saves parameters while scaling compute. The cost of the parameter saving is reduced capacity. Zhu et al. (2025) show that looped models match standard transformers on knowledge manipulation but not on per-parameter memorisation, and Frey et al. (2026) report a corresponding empirical pattern downstream: adaptive looping improves mathematical reasoning but leaves commonsense benchmarks largely flat. Both observations show that looping buys compute at the cost of capacity.

Per-token compute allocation. A separate line of work allocates compute adaptively at the token level. Mixture-of-Experts (Shazeer et al., 2017; Fedus et al., 2022) routes each token to a small subset of many parallel experts of the same shape, decoupling parameter count from per-token compute. Mixture-of-Depths (Raposo et al., 2024) routes tokens to skip or apply a layer, varying effective depth per position. Mixture-of-Recursions (Bae et al., 2025) extends this to looped stacks by varying the number of shared-block applications per token. All of these route along a single axis (which experts, how many loop iterations, or whether to apply a layer at all). While MoE and our dual-path block both attach a learned router to a transformer layer, they route over different sets of options. In MoE, the router selects among N feed-forward experts that share the same architecture but hold different learned weights; the choice is over which parameters a token sees. In the dual-path block, the

router weighs two sublayers that differ in kind: one is a shared-parameter sublayer applied K times, the other is a wider sublayer applied once. The choice is instead over what type of update a token receives. Furthermore, MoE routers are top- k sparse, whereas our gate is dense. Because both paths are always evaluated in our block, we do not skip compute; we re-allocate it. This also means both updates are observed at every token and every layer, making the gate’s value a direct read-out of how the trained model chose to allocate between two options that were both processed. Finally, because the two mechanisms target different axes, they are compositional rather than competing. In theory, a MoE layer could be placed inside the wide path of a dual-path block, with the gate selecting whether to route a token through looped compute or through routed capacity.

Memory-augmented transformers. A complementary route to recovering capacity in parameter-shared models is to attach learned memory banks the model can query, as in product-key memory layers (Lample et al., 2019) and persistent memory in attention (Sukhbaatar et al., 2019). Frey et al. (2026) combine adaptive looping with per-layer and global memory banks and find that memory closes part of the commonsense gap that looping alone cannot bridge. The dual-path block addresses the same capacity bottleneck from the architectural side: rather than adding a separately queried memory module that scales weakly, it adds a parallel wide FFN sublayer inside each layer and lets a per-token gate decide how much of each token’s update comes from looped compute vs. wider parameters.

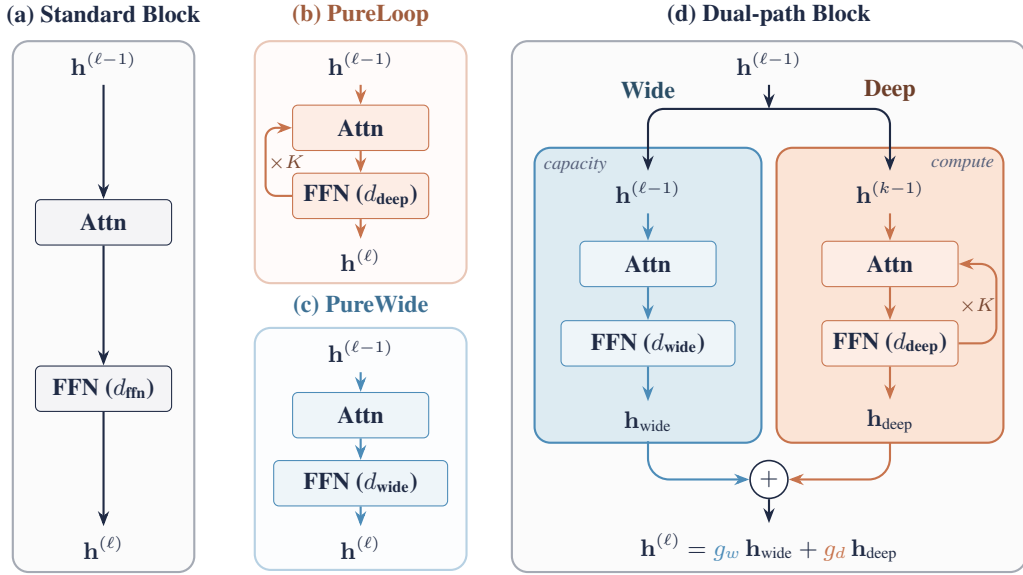
3 Method

3.1 Problem statement and notation

Scaling a transformer layer generally involves either expanding *capacity* (adding parameters, typically via a wider feed-forward network) or extending *compute* (increasing sequential operations on the hidden state, usually via more layers or by recursively re-applying a shared one). We study an architecture that exposes the two axes *separately within each layer* and let the model decide, per token, how to allocate between them.

3.2 Baseline

Given an input tensor $x \in \mathbb{R}^{B \times T \times d}$, where B denotes the batch size, T represents the sequence



Per-token allocation

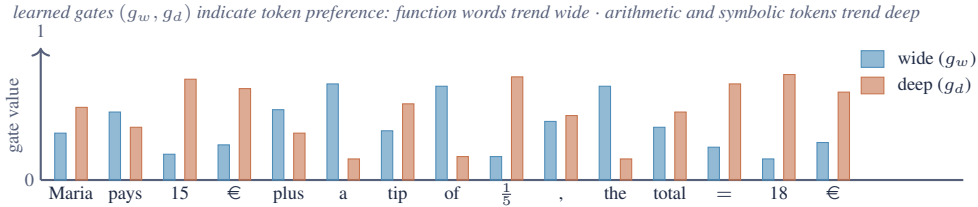


Figure 1: Block architectures. (a) Standard transformer block. (b) PURELOOP: a shared block re-applied K times. (c) PUREWIDE: a single block with enlarged FFN. (d) Dual-path block, which runs (c) and (b) in parallel on the same input and combines them via two per-token sigmoid gates g_w, g_d . Bottom panel: schematic of the learned gates across sequence tokens.

length, and d is the model dimension, a standard transformer sublayer Φ is defined as

$$u = x + s \cdot \text{Attn}(\text{RMSNorm}(x)),$$

$$\Phi(x; s) = u + s \cdot \text{FFN}(\text{RMSNorm}(u)), \quad (1)$$

where $s \in \mathbb{R}_{>0}$ is a scalar gain on the sublayer contribution. In a standard transformer $s = 1$; in our dual-path block, s is learned per recursion step and per path.

3.3 Dual-path block

Each block exposes the two scaling axes as two parallel sublayers that share the same input x , as illustrated in Figure 1. One sublayer adds sequential compute by re-applying itself K times with shared parameters; the other adds capacity by using a wider FFN and is applied once. A per-token gate combines them.

Deep path (compute). The deep sublayer Φ_{deep} uses the FFN hidden dimension d_{deep} and is applied

K times iteratively with shared parameters:

$$h^{(k)} = \Phi_{\text{deep}}\left(h^{(k-1)}; s_d^{(k)}\right), \quad (2)$$

where $h^{(0)} = x$ and $k = 1, \dots, K$. The per-step gains $s_d^{(k)} = \text{softplus}(\alpha^{(k)})$ are learned, with one $\alpha^{(k)}$ per step. Initialising $\alpha^{(k)} = -7$ gives $s_d^{(k)} \approx 9 \times 10^{-4}$, so the recursion begins as a near-identity and the model learns step-wise deviations from x .

Rather than returning $h^{(K)}$ directly, the deep path is a learned weighted combination of all intermediate states. A small router (a linear projection from the current state $h^{(k)}$ and a normalised step index $k/(K-1)$) produces a per-step weight $q_k \in [0, 1]$. Letting $\pi_k = \prod_{j < k} (1 - q_j)$, the deep representation is

$$h_{\text{deep}} = \sum_{k=1}^{K-1} \pi_k q_k h^{(k)} + \pi_K h^{(K)}. \quad (3)$$

The router thus lets the model down-weight later loop iterations on a per-token basis.

Wide path (capacity). The wide sublayer Φ_{wide} has the same attention configuration as Φ_{deep} but an enlarged FFN hidden dimension $d_{\text{wide}} > d_{\text{deep}}$, and is applied once:

$$h_{\text{wide}} = \Phi_{\text{wide}}(x; s_w), \quad s_w = \text{softplus}(\beta). \quad (4)$$

The scalar β is initialised to -7 , matching the deep path. This path adds parameters through the wider FFN but no sequential compute beyond a normal layer.

Per-token gating. A linear projection $W_g \in \mathbb{R}^{d \times 2}$ with bias $b_g \in \mathbb{R}^2$ maps the layer input to logits $(\ell_d, \ell_w) = xW_g + b_g$, giving two independent sigmoid gates $g_d = \sigma(\ell_d)$ and $g_w = \sigma(\ell_w)$, both in $[0, 1]^{B \times T}$. The combined update is

$$y = g_d \odot h_{\text{deep}} + g_w \odot h_{\text{wide}}. \quad (5)$$

We initialise W_g and b_g to zero, so each token receives $g_d = g_w = 0.5$ at the start of training. The gate is the mechanism by which the model can route tokens that benefit from compute toward the deep path and tokens that benefit from capacity toward the wide path.

Single-axis baselines. Disabling one path reduces a block to a *looped* (PURELOOP) layer ($y = h_{\text{deep}}$, K recursions of the standard FFN; Figure 1b) or a *width-scaled* (PUREWIDE) layer ($y = h_{\text{wide}}$, one pass of the enlarged FFN; Figure 1c). These two configurations share the backbone, data, and recipe with the dual-path block and put the entire per-layer FFN FLOP budget on one axis. PUREWIDE has the largest parameter count within a budget (no parameter sharing across recursion); PURELOOP has the smallest (one FFN re-applied K times).

3.4 Routing read-outs

Because both paths are evaluated for every token (Section 3.3), the forward pass exposes the raw gates (g_d, g_w) and the per-path update vectors $\Delta_d = h_{\text{deep}} - x$ and $\Delta_w = h_{\text{wide}} - x$ at every layer and every token.

The raw gate value alone ignores update size. We therefore report the fraction of the residual update that came from the deep path,

$$\rho_d = \frac{g_d \|\Delta_d\|}{g_d \|\Delta_d\| + g_w \|\Delta_w\|} \in [0, 1], \quad (6)$$

computed per token per layer. $\rho_d = 1$ means the entire update at that position came from the deep

path; $\rho_d = 0$ means it came entirely from the wide path; $\rho_d = 0.5$ is balanced. We refer to ρ_d as the *deep share* throughout.

Path alignment. We also record the cosine similarity between the two path deltas,

$$\cos(\Delta_d, \Delta_w) = \frac{\Delta_d \cdot \Delta_w}{\|\Delta_d\| \|\Delta_w\|}. \quad (7)$$

A value near $+1$ means the two paths push the residual in the same direction, i.e. deep and wide path do the same, while a value near 0 means they push in orthogonal directions.

4 Experiments

The backbone is a GPT2-style (Radford et al., 2019) decoder-only transformer with $L = 16$ layers, hidden dimension $d = 768$, and 12 attention heads. Attention uses rotary positional embeddings (Su et al., 2024b) applied to queries and keys, with RMSNorm on queries and keys prior to attention (Dehghani et al., 2023). Feed-forward sublayers are SwiGLU (Shazeer, 2020). These parameters are held fixed across every configuration in the paper, including the single-axis controls; only the FFN widths and the per-layer recursion depth vary.

4.1 Setup

Models and configurations. We train models at two iso-FLOP budgets, specified by the per-layer FFN FLOPs per token ($F_M = 80\text{M}$ and $F_M = 160\text{M}$, corresponding to $\sim 1.28\text{G}$ and $\sim 2.56\text{G}$ total FLOPs per token for a 16-layer model). The detailed procedure for solving for matched FFN widths is given in Appendix B. Within each budget we sweep the dual-path FFN allocation $\alpha \in \{25, 50, 75\}$ (the share of FFN FLOPs spent on the deep path) and the recursion depth $K \in \{2, 3, 4\}$. At fixed budget, larger K and larger α reduce parameter count, since both shift compute toward the shared-parameter deep path. Unique parameter counts across all configurations span from roughly 240M up to 1.4B. All models share pre-RMSNorm (Zhang and Sennrich, 2019), RoPE (Su et al., 2024b), SwiGLU (Shazeer, 2020) and QK-norm (Henry et al., 2020). Exact $L, d, h_q, h_{kv}, d_{\text{ffn}}, d_{\text{ffn}}^{\text{wide}}$ per configuration are listed in Appendix C (Tables 2 and 3).

Data and training. All models are trained on a deduplicated subset of Nemotron-CC (Su et al., 2024a) for 38B tokens with the GPT-2

Table 1: **Main results.** Iso-FLOP comparison at two budgets. DUAL configurations use `loop=4`; rows vary the FFN FLOP allocation between the deep and wide paths ($a_{25}/a_{50}/a_{75} = 25/50/75\%$ on the deep path). The full sweep over loop depths is in Appendix C. Params is shown relative to PUREWIDE within each budget. All rows within a budget are matched in FLOPs.

Configuration	Params	FLOPs	Language modelling		Commonsense		Math	
			C4 ↓	Wiki ↓	Acc. ↑	BPB ↓	Acc. ↑	BPB ↓
PUREWIDE	719M (1.00×)	80M	1.037	0.946	0.5203	0.9920	0.0791	0.5261
PURELOOP								
Loop=2	398M (0.55×)	80M	1.051	0.961	0.5036	1.0028	0.0723	0.5372
Loop=3	294M (0.41×)	80M	1.065	0.976	0.5067	1.0236	0.0723	0.5454
Loop=4	238M (0.33×)	80M	1.078	0.992	0.5031	1.0352	0.0527	0.5564
DUALPATH (<i>ours</i>)								
$\alpha = 25$	606M (0.84×)	80M	1.037	0.942	0.5163	0.9902	0.0664	0.5253
$\alpha = 50$	483M (0.67×)	80M	1.036	0.939	0.5256	0.9820	0.0898	0.5198
$\alpha = 75$	360M (0.50×)	80M	1.045	0.948	0.5249	0.9892	0.0918	0.5227
PUREWIDE	1361M (1.00×)	160M	1.018	0.922	0.5384	0.9636	0.1250	0.5077
PURELOOP								
Loop=2	719M (0.53×)	160M	1.027	0.931	0.5303	0.9814	0.1045	0.5091
Loop=3	502M (0.37×)	160M	1.037	0.939	0.5244	0.9894	0.1191	0.5150
Loop=4	398M (0.29×)	160M	1.045	0.945	0.5137	1.0010	0.0938	0.5199
DUALPATH (<i>ours</i>)								
$\alpha = 25$	1125M (0.83×)	160M	1.013	0.911	0.5420	0.9610	0.1250	0.5066
$\alpha = 50$	880M (0.65×)	160M	1.017	0.920	0.5326	0.9704	0.1328	0.4959
$\alpha = 75$	644M (0.47×)	160M	1.021	0.924	0.5335	0.9700	0.1406	0.5047

tokenizer. Sequence length is 4096. We use the `modalities` training framework (Lübbering et al., 2026) using the AdamW optimizer (with peak learning rate 5×10^{-4} , a linear warmup of 184 steps, and a cosine decay schedule down to 5×10^{-5}). Wall-clock training times range from 12.8 to 21.4 hours per model across 64 GPUs. Full optimizer hyperparameters are listed in Appendix A.

Baselines. We compare against two iso-FLOP single-axis controls, trained with the same backbone, data, and recipe:

- PUREWIDE (L layers, single wider FFN of width $d_{\text{ffn}}^{\text{wide}}$, no recursion): our block with the deep path disabled. Spends the entire per-layer FFN FLOP budget on capacity.
- PURELOOP (L layers, standard FFN width, recursion depth K , no wide path): our block with the wide path disabled. Spends the entire per-layer FFN FLOP budget on sequential compute.

Evaluation. We report bits-per-byte (BPB) on Paloma C4 and WikiText-103 for language modelling, mean accuracy and BPB on six commonsense tasks (ARC-c, ARC-e, HellaSwag, PIQA, SIQA, WinoGrande), GSM8k accuracy and the

OLMo3 base-easy math BPB average over seven sub-tasks, and LAMBADA / QASPER for reading and QA. BPB rather than accuracy gives finer-grained signal for these pre-training scales. Full per-task numbers are in Appendix E (Tables 5 and 6).

4.2 Main results

Table 1 reports our main comparison at both FLOP budgets.

A dual-path configuration performs best at both budgets. We focus on $K=4$ throughout this section, matching the configurations shown in Table 1 (see Appendix E for the full results). At both FLOP budgets, a dual-path configuration beats both single-axis controls on aggregate BPB (the mean of C4, WikiText-103, commonsense, and math BPB). At $F_M = 80\text{M}$, $\alpha = 50$ (483M params, $0.67\times$ PUREWIDE) achieves the best aggregate BPB (0.8693 vs. 0.8753 for PUREWIDE and 0.8880 for the best PURELOOP), and is also best on C4, Wiki, commonsense BPB, math BPB, and commonsense accuracy. At $F_M = 160\text{M}$, the optimum shifts toward capacity: $\alpha = 25$ (1125M params, $0.83\times$ PUREWIDE) is best on aggregate BPB (0.8478 vs. 0.8530 for PUREWIDE and 0.8622 for the best PURELOOP), and wins C4, Wiki, commonsense BPB, and commonsense ac-

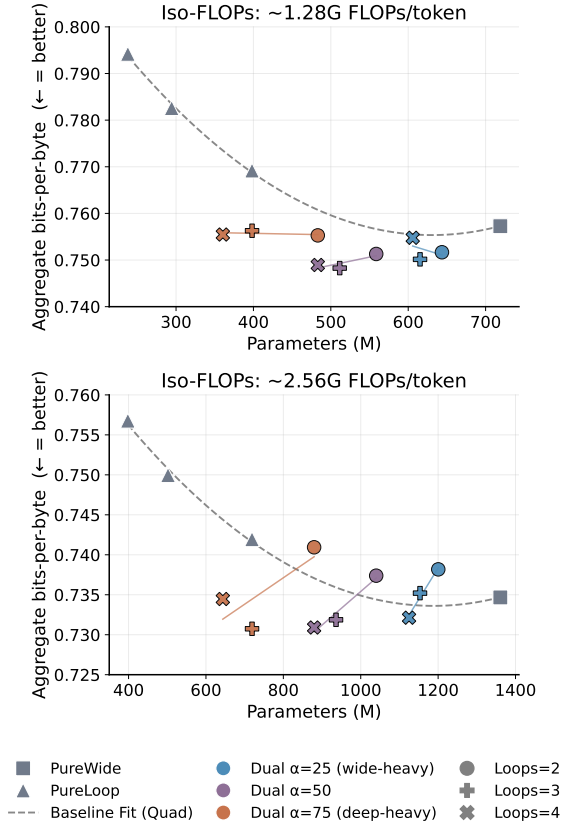


Figure 2: **Parameter scaling sweep of dual-path configurations** compared against PUREWIDE and PURELOOP controls at matched FLOP budgets. Number of Loops for PURELOOP (triangle) is $K=2, 3, 4$ (from left to right). Note that PUREWIDE is equivalent to PURELOOP with $K=1$ but without additional routing overhead.

curacy. This shift toward capacity at the higher budget is consistent with the broader picture that looped (parameter-shared) compute is parameter-bottlenecked.

Allocation between deep and wide path. We now investigate how the model performance changes when varying α within the $K=4$ models. Capacity-heavy configurations ($\alpha = 25$) are strongest on language modelling and commonsense: at $F_M = 160M$, $\alpha=25$ gives the best C4 and WikiText-103 BPB and the best commonsense accuracy and BPB. Compute-heavy configurations ($\alpha = 75$) are strongest on math: GSM8k accuracy peaks at $\alpha=75$ at both budgets (0.0918 at $F_M = 80M$, 0.1406 at $F_M = 160M$). This shows, that shifting FFN FLOPs toward the wide path adds parameters and helps knowledge-heavy tasks, while shifting them toward the deep path adds sequential compute and helps reasoning-heavy tasks.

Pareto position in the parameter–quality plane.

We next plot aggregated bits-per-byte against parameter count for all configurations ($K \in \{2, 3, 4\}$ and $\alpha \in \{25, 50, 75\}$) in Figure 2. For optimal parameter efficiency at a fixed FLOP budget, a model should land in the lower left corner. The dashed curve is a quadratic fit through the single-axis controls (the three PURELOOP points and PUREWIDE) and traces the Pareto frontier reachable by sweeping the wide/loop allocation in a standard transformer. Within each α , connecting $K \in \{2, 3, 4\}$ traces a short per- α segment moving from right to left (as higher K reduces parameter count at fixed FLOPs). At the lower budget ($F_M = 80M$, $\sim 1.28G$ FLOPs), the segments have different slopes, with some increasing performance along the line while others remain flat. However, at the higher budget ($F_M = 160M$, $\sim 2.56G$ FLOPs), increasing the loop count generally improves performance across all α values, driving the models further into the optimal lower-left region.

4.3 Where does the model spend its budget?

Having established that the dual-path block improves overall performance, we now examine the learned gates to understand how the model allocates its budget. Because the architecture evaluates both paths densely, we can directly read out the routing decisions and residual updates at inference time to uncover the model’s underlying preferences for sequential compute (the deep path) or parameter capacity (the wide path). We find that the routing preference varies a) across the layer’s position in the stack, b) the identity of the token (e.g. noun vs. number), and c) the task the token is part of (math vs. question answering). All analyses below use the balanced $\alpha = 50$, $K = 4$ model evaluated on three Paloma sources (WikiText-103, TriviaQA, GSM8K).

Depth in the stack. Figure 4(a) plots the mean deep share per layer for all three $K \in \{2, 3, 4\}$ models at $\alpha = 50$, along with their average. Two regimes are visible. The middle of the network (L2–L9) is wide-dominated, with deep share between 0.28 and 0.40, while the last two layers (L14–L15) flip to deep-dominated, with the average rising to 0.5–0.6. The pattern is consistent across loop counts, so the shape reflects the layer’s role in the stack rather than the specific recursion depth.

Panel (b) shows the mean cosine similarity be-

tween the update vectors from the deep path (Δ_d) and the wide path (Δ_w) at each layer. A value near +1 means the paths produce nearly identical updates (and one is redundant), a value near 0 means they push in orthogonal directions (the paths contribute non-overlapping information). We observe mostly low values across the middle of the network, indicating that the deep and wide paths are processing the same input in genuinely different ways rather than producing scaled copies of one another.

Task. The gate responds to the task a token is part of. Figure 5 shows two example sequences side by side: in the GSM8K answer, numbers and arithmetic operators (15, *, =, 3, 18) are deep-leaning, and the deep preference strengthens through the arithmetic blocks. In the TriviaQA example, the answer token `Oxy` is the most deep-leaning position in the sequence, while the surrounding question words sit on the wide side.

Figure 6 resolves the same examples layer by layer and shows the depth pattern from earlier: later layers prefer the deep path, mid layers prefer the wide path. For a population estimate we align one thousand samples from each task to the `Answer` token and plot the per-layer difference $\rho_d^{\text{GSM8K}} - \rho_d^{\text{TriviaQA}}$ (Figure 6c). Alignment to a shared anchor is needed because the `Answer` token sits at different absolute positions in sequences of varying length. The post-`Answer` positions in GSM8K are markedly more deep-leaning than the corresponding TriviaQA positions in the late layers. At the same depth and the same relative position, a reasoning task routes more deeply than a knowledge task.

Token identity. To investigate in more detail beyond task identity we tag every token with its Universal POS tag (Petrov et al., 2012; Nivre et al., 2016) using spaCy (Honnibal et al., 2020) (`en_core_web_sm`) on the decoded text, with a regex override for arithmetic tokens (digits, operators, =, <<, >>, #####). Each model token inherits the tag of the character span it overlaps most. Figure 7 plots, for every (POS, layer) pair, the mean deep share over all tokens with that tag, restricted to tags with at least 10 occurrences. The ordering is stable across all three datasets and visible in the boxplot of panel (e): `SPACE`, `PUNCT` (e.g., `,`, `.`), and `SYM` (e.g., `=`, `-`, `<<`) receive the highest deep share; `ADV` (e.g., `also`, `as`), `PART` (e.g., `to`, `'s`), `PRON` (e.g., `he`, `it`), `ADJ` (e.g., `many`, `first`),

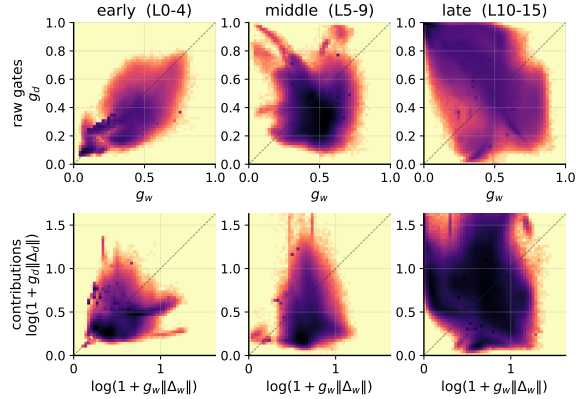


Figure 3: **Joint 2D density of routing gates and update contributions**, split into layer bands (early, middle, late) and averaged across three Paloma datasets (`wikitext_103`, `triviaqa`, `gsm8k`). Row A plots the joint density of the raw gates selected by the router: deep gate g_d on the y-axis and wide gate g_w on the x-axis in $[0, 1]^2$. Row B plots the joint density of update contributions on a log-transformed scale: $\log(1 + g_w \|\Delta_w\|)$ (wide contribution) vs. $\log(1 + g_d \|\Delta_d\|)$ (deep contribution), which shows the actual magnitude of vectors added to the residual stream.

and `VERB` (e.g., `made`, `used`) receive the lowest; `NUM` (e.g., `2`, `5`) and `NOUN` (e.g., `Question`, `Answer`) sit in the middle. Overall, the POS pattern follows an interpretable split: symbolic and structural tokens (`SPACE`, `PUNCT`, `SYM`) route to compute, while lexical content tokens (`VERB`, `ADJ`, `ADV`, `PRON`, `PART`), route to capacity.

Per-token decisions become more polarised with depth. The analyses so far show *what* the gate prefers but not *how strongly* it commits to those preferences. We therefore plot the joint distribution of the two gates. Figure 3 plots the 2D density of (g_w, g_d) pooled across all tokens, grouped into three layer bands (early L0–4, middle L5–9, late L10–15). The dashed diagonal marks equal routing ($g_d = g_w$): mass on the diagonal corresponds to balanced mixtures, while mass off the diagonal corresponds to tokens that commit primarily to one path. The per-layer breakdown is shown in Appendix Figure 8. We observe that the density moves off the diagonal as depth increases. Early layers (L0–4) concentrate in a narrow band along the positive diagonal near the origin, indicating small and roughly balanced gates for most tokens. Late layers (L10–15) push density onto the boundaries with a cluster near $g_d \rightarrow 1$ (tokens routed almost entirely through the deep path) and a cluster near $g_w \rightarrow 1$ (tokens routed almost entirely through

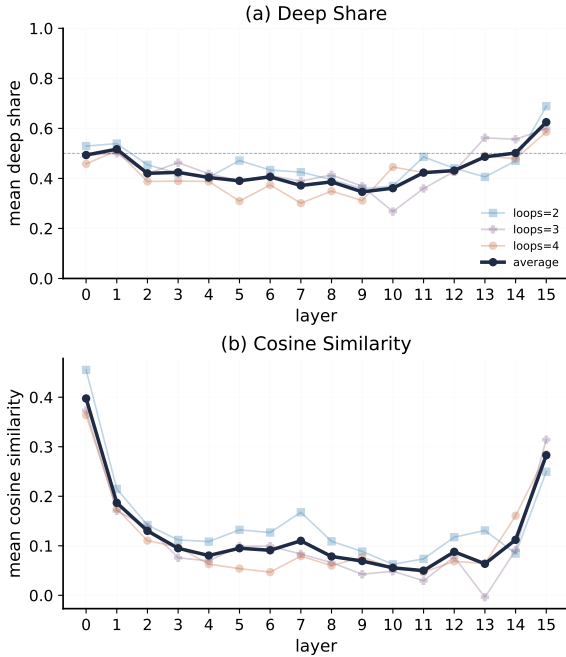


Figure 4: **Routing share and update vector alignment across layers.** Panel (a) shows the mean routing deep share per layer. Low value indicates preference for the wide path, high values for the deep path. Panel (b) shows the mean cosine similarity between the update vector from the deep path (Δ_d) and that from the wide path (Δ_w) at each layer. Low values indicate that the deep and wide path process the same input differently.

the wide path) Row B plots the same density after re-weighting each axis by the actual update magnitude ($\log(1 + g_w \|\Delta_w\|)$ vs. $\log(1 + g_d \|\Delta_d\|)$), which accounts for the fact that a high gate value contributes little if its path’s update is small. We observe, that the gate is not just choosing different mixtures for different tokens but it also commits more strongly to one path or the other as the residual stream moves through the network.

5 Conclusion

Standard transformer layers conflate two distinct scaling axes: compute (sequential operations on a hidden state) and capacity (parameters available at a single step). The dual-path block separates them, using a recursive deep sublayer and a parallel wider sublayer combined by a dense learned gate. At two iso-FLOP budgets, the best dual-path configuration Pareto-dominates both single-axis controls on aggregate language modelling, commonsense, and math metrics while using fewer parameters than the width-scaled baseline. The ratio between the wide and deep path α provides a predictable trade-off, with capacity-heavy settings favoring knowledge

tasks and compute-heavy settings favoring reasoning.

Our results show that this parallel formulation can outperform iso-FLOP single-axis baselines on aggregate language modelling, commonsense, and math metrics at two FLOP budgets. Because both paths are evaluated at every token, the routing decisions are a direct read-out of how the trained model chose to spend its budget, not a sampling artifact. This learned allocation is interpretable. It varies systematically with layer depth, with wide being preferred in the middle of the stack, and deep dominated in the last two layers. Moreover, function words and lexical content trend wide while punctuation, symbols, and arithmetic tokens trend deep.

The dual-path block opens several directions we find promising. First, our experiments cover two FLOP budgets on a single 16-layer backbone. The per- α trajectories in Figure 2 steepen from the lower to the higher budget, hinting that the gains from separating the two axes may compound rather than plateau with scale. Confirming this at billion-parameter budgets and across different depth/width ratios is the most direct extension.

Second, as noted above, the dual-path gate and MoE routing target orthogonal axes and are architecturally compositional: loops increase FLOPs while keeping parameters the same, while MoEs increase the parameters while keeping FLOPs fixed (with fixed top-k). In our model a MoE layer could occupy the wide path, with the outer gate deciding between looped compute and routed capacity.

These directions suggest that separating compute and capacity within a layer is a primitive that naturally combines with other scaling ideas and yields an interpretable signal as a free byproduct.

References

- Sangmin Bae, Yujin Kim, Reza Bayat, Sungnyun Kim, Jiyoun Ha, Tal Schuster, Adam Fisch, Hrayr Harutyunyan, Ziwei Ji, Aaron Courville, and 1 others. 2025. Mixture-of-recursions: Learning dynamic recursive depths for adaptive token-level computation. *arXiv preprint arXiv:2507.10524*.
- Andrea Banino, Jan Balaguer, and Charles Blundell. 2021. Pondernet: Learning to ponder. *arXiv preprint arXiv:2107.05407*.
- Mostafa Dehghani, Josip Djolonga, Basil Mustafa, Piotr Padlewski, Jonathan Heek, Justin Gilmer, Andreas Peter Steiner, Mathilde Caron, Robert Geirhos, Ibrahim Alabdulmohsin, and 1 others. 2023. Scaling

- vision transformers to 22 billion parameters. In *International Conference on Machine Learning*, pages 7480–7512. PMLR.
- Mostafa Dehghani, Stephan Gouws, Oriol Vinyals, Jakob Uszkoreit, and Łukasz Kaiser. 2019. Universal transformers. In *International Conference on Learning Representations*.
- William Fedus, Barret Zoph, and Noam Shazeer. 2022. Switch transformers: Scaling to trillion parameter models with simple and efficient sparsity. *Journal of Machine Learning Research*, 23(120):1–39.
- Markus Frey, Behzad Shomali, Ali Hamza Bashir, David Berghaus, Joachim Koehler, and Mehdi Ali. 2026. Adaptive loops and memory in transformers: Think harder or know more? In *Latent & Implicit Thinking Workshop @ ICLR*.
- Jonas Geiping, Sean McLeish, Neel Jain, John Kirchenbauer, Siddharth Singh, Brian R Bartoldson, Bhavya Kailkhura, Abhinav Bhatele, and Tom Goldstein. 2025. Scaling up test-time compute with latent reasoning: A recurrent depth approach. *arXiv preprint arXiv:2502.05171*.
- Alex Graves. 2016. Adaptive computation time for recurrent neural networks. *arXiv preprint arXiv:1603.08983*.
- Yuling Gu, Oyvind Tafjord, Bailey Kuehl, Dany Hadad, Jesse Dodge, and Hannaneh Hajishirzi. 2025. Olmes: A standard for language model evaluations. In *Findings of the Association for Computational Linguistics: NAACL 2025*, pages 5005–5033.
- Alex Henry, Prudhvi Raj Dachapally, Shubham Vivek Pawar, and Yuxuan Chen. 2020. Query-key normalization for transformers. In *Findings of the Association for Computational Linguistics: EMNLP 2020*, pages 4246–4253.
- Matthew Honnibal, Ines Montani, Sofie Van Landeghem, and Adriane Boyd. 2020. `spacy: Industrial-strength natural language processing in python`.
- Ahmadreza Jeddi, Marco Ciccone, and Babak Taati. 2026. Loopformer: Elastic-depth looped transformers for latent reasoning via shortcut modulation. *arXiv preprint arXiv:2602.11451*.
- Guillaume Lample, Alexandre Sablayrolles, Marc’Aurelio Ranzato, Ludovic Denoyer, and Hervé Jégou. 2019. Large memory layers with product keys. *Advances in Neural Information Processing Systems*, 32.
- Max Lübbering, Timm Ruland, Richard Rutmann, Felix Stollenwerk, David Fitzek, Michael Fromm, Alexander Weber, Rafet Sifa, Nicolas Flores-Herr, Joachim Köhler, and 1 others. 2026. Modalities, a pytorch-native framework for large-scale LLM training and research. *arXiv preprint*.
- Joakim Nivre, Marie-Catherine de Marneffe, Filip Ginter, Yoav Goldberg, Jan Hajič, Christopher D Manning, Ryan McDonald, Slav Petrov, Sampo Pyysalo, Natalia Silveira, Reut Tsarfaty, and Daniel Zeman. 2016. Universal dependencies v1: A multilingual treebank collection. In *Proceedings of the Tenth International Conference on Language Resources and Evaluation (LREC’16)*, pages 1659–1666.
- Slav Petrov, Dipanjan Das, and Ryan McDonald. 2012. A universal part-of-speech tagset. In *Proceedings of the Eighth International Conference on Language Resources and Evaluation (LREC’12)*, pages 2089–2096.
- Alec Radford, Jeffrey Wu, Rewon Child, David Luan, Dario Amodei, and Ilya Sutskever. 2019. Language models are unsupervised multitask learners. *OpenAI Technical Report*.
- David Raposo, Sam Ritter, Blake Richards, Timothy Lillicrap, Peter Conway Humphreys, and Adam Santoro. 2024. Mixture-of-depths: Dynamically allocating compute in transformer-based language models. *arXiv preprint arXiv:2404.02258*.
- Nikunj Saunshi, Nishanth Dikkala, Zhiyuan Li, Sanjiv Kumar, and Sashank J Reddi. 2025. Reasoning with latent thoughts: On the power of looped transformers.
- Noam Shazeer. 2020. GLU variants improve transformer. *arXiv preprint arXiv:2002.05202*.
- Noam Shazeer, Azalia Mirhoseini, Krzysztof Maziarz, Andy Davis, Quoc Le, Geoffrey Hinton, and Jeff Dean. 2017. Outrageously large neural networks: The sparsely-gated mixture-of-experts layer. In *International Conference on Learning Representations*.
- Dan Su, Kezhi Kong, Ying Lin, Joseph Jennings, Brandon Norick, Markus Kliegl, Mostofa Patwary, Mohammad Shoeybi, and Bryan Catanzaro. 2024a. Nemotron-CC: Transforming Common Crawl into a refined long-horizon pretraining dataset. *arXiv preprint arXiv:2412.02595*.
- Jianlin Su, Yu Lu, Shengfeng Pan, Ahmed Murtadha, Bo Wen, and Yunfeng Liu. 2024b. Roformer: Enhanced transformer with rotary position embedding. *Neurocomputing*, 568:127063.
- Sainbayar Sukhbaatar, Edouard Grave, Guillaume Lample, Herve Jegou, and Armand Joulin. 2019. Augmenting self-attention with persistent memory. *arXiv preprint arXiv:1907.01470*.
- Biao Zhang and Rico Sennrich. 2019. Root mean square layer normalization. In *Advances in Neural Information Processing Systems*, volume 32.
- Rui-Jie Zhu, Zixuan Wang, Kai Hua, Tianyu Zhang, Ziniu Li, Haoran Que, Boyi Wei, Zixin Wen, Fan Yin, He Xing, and 1 others. 2025. Scaling latent reasoning via looped language models. *arXiv preprint arXiv:2510.25741*.

Appendix

A Training Details

All models are trained using the `modalities` framework. We use the AdamW optimizer with $\beta_1 = 0.9$, $\beta_2 = 0.95$, $\epsilon = 10^{-8}$, and weight decay of 0.3 (excluding embedding and RMSNorm layers). The learning rate is warmed up linearly from 5×10^{-6} to a peak of 5×10^{-4} over 184 steps, and then decayed to 5×10^{-5} using a cosine annealing schedule. Wall-clock training times range from 12.8 to 21.4 hours per model (average of 16.0 hours) on the cluster hardware. Total pretraining tokens are 38B.

B FLOP-matching protocol

The FLOP budget F_M is the per-token, per-layer FFN compute. For each configuration we solve for the largest legal d_{ffn} (and, for dual-path, $d_{\text{ffn}}^{\text{wide}}$) whose induced h_{eff} keeps the per-layer FFN cost at or below F_M , also accounting for the router on the dual-path block. Within each budget the controls and the dual configurations agree on total per-token FFN FLOPs to within 0.5%; the same backbone ($L = 16$, $d = 768$, $h_q = h_{kv} = 12$) is held fixed across all configurations, so attention compute is identical.

This appendix gives the exact accounting used to match FLOPs across configurations. All FLOPs are reported per token and per layer.

Per-sublayer FLOPs. Let d be the model dimension, $n_{\text{rep}} = h_q/h_{kv}$ the repeat factor (1 in all our runs), and d_{ffn} the *configured* FFN hidden width. The SwiGLU *effective* hidden width used by the model is

$$h_{\text{eff}}(d_{\text{ffn}}) = 64 \cdot \left\lceil \frac{1}{64} \lceil 2d_{\text{ffn}}/3 \rceil \right\rceil, \quad (8)$$

i.e. the LLaMA-style 2/3 scaling rounded up to a multiple of 64. The per-token FLOPs of one sublayer are

$$\text{FLOP}_{\text{attn}} = 4d^2 + 4d^2/n_{\text{rep}}, \quad (9)$$

$$\text{FLOP}_{\text{ffn}}(d_{\text{ffn}}) = 6d \cdot h_{\text{eff}}(d_{\text{ffn}}). \quad (10)$$

The dual-path two-gate router contributes $\text{FLOP}_{\text{gate}} = 4d$ FLOPs per token (linear $d \rightarrow 2$).

Per-layer FLOP budgets. For the three layer types, the per-layer FFN-side FLOP count F_M

Config	K	d_{ffn}	$d_{\text{ffn}}^{\text{wide}}$	Params	Time
PUREWIDE	1	—	24576	719M	17.6h
PURELOOP $K=2$	2	11392	—	398M	15.2h
PURELOOP $K=3$	3	7104	—	294M	16.6h
PURELOOP $K=4$	4	4864	—	238M	15.9h
DUAL $\alpha=25, K=2$	2	1600	17920	644M	14.6h
DUAL $\alpha=25, K=3$	3	576	17920	615M	14.7h
DUAL $\alpha=25, K=4$	4	64	17920	606M	12.8h
DUAL $\alpha=50, K=2$	2	4864	11392	559M	17.4h
DUAL $\alpha=50, K=3$	3	2752	11392	511M	17.0h
DUAL $\alpha=50, K=4$	4	1600	11392	483M	16.5h
DUAL $\alpha=75, K=2$	2	8128	4864	483M	14.2h
DUAL $\alpha=75, K=3$	3	4864	4864	398M	13.3h
DUAL $\alpha=75, K=4$	4	3264	4864	360M	14.3h

Table 2: Per-configuration widths, parameter counts, and wall-clock training times at the $F_M = 80\text{M}$ FFN-FLOP budget.

Config	K	d_{ffn}	$d_{\text{ffn}}^{\text{wide}}$	Params	Time
PUREWIDE	1	—	50624	1361M	21.4h
PURELOOP $K=2$	2	24448	—	719M	19.9h
PURELOOP $K=3$	3	15744	—	502M	15.5h
PURELOOP $K=4$	4	11392	—	398M	17.7h
DUAL $\alpha=25, K=2$	2	4864	37440	1200M	14.8h
DUAL $\alpha=25, K=3$	3	2752	37440	1153M	15.1h
DUAL $\alpha=25, K=4$	4	1600	37440	1125M	15.0h
DUAL $\alpha=50, K=2$	2	11392	24448	1040M	21.3h
DUAL $\alpha=50, K=3$	3	7104	24448	936M	15.6h
DUAL $\alpha=50, K=4$	4	4864	24448	880M	19.0h
DUAL $\alpha=75, K=2$	2	17920	11392	880M	13.2h
DUAL $\alpha=75, K=3$	3	11392	11392	719M	14.5h
DUAL $\alpha=75, K=4$	4	8128	11392	644M	13.1h

Table 3: Per-configuration widths, parameter counts, and wall-clock training times at the $F_M = 160\text{M}$ FFN-FLOP budget.

(which we hold fixed at 80M or 160M) is

$$F_M^{\text{PUREWIDE}} = \text{FLOP}_{\text{attn}} + \text{FLOP}_{\text{ffn}}(d_{\text{ffn}}^{\text{wide}}), \quad (11)$$

$$F_M^{\text{PURELOOP}} = K(\text{FLOP}_{\text{attn}} + \text{FLOP}_{\text{ffn}}(d_{\text{ffn}})), \quad (12)$$

$$F_M^{\text{DUAL}} = K(\text{FLOP}_{\text{attn}} + \text{FLOP}_{\text{ffn}}(d_{\text{ffn}})) + \text{FLOP}_{\text{attn}} + \text{FLOP}_{\text{ffn}}(d_{\text{ffn}}^{\text{wide}}) + \text{FLOP}_{\text{gate}}. \quad (13)$$

The dual-path layer therefore pays an extra attention pass and a small router term relative to a single-axis layer at the same FFN FLOPs. Note that we hold all FLOPs fixed at 80M or 160M per layer and per token by adjusting the size of the FFN.

Solving for FFN widths. Given F_M , K , and (for dual) a deep-FLOP fraction $\alpha \in (0, 1)$, we

GSM8K Mathematical Reasoning Example

Question : Ashley’s pizza delivery costs \$15. What is the total amount that Ashley should give the delivery man if she wants to give a tip that is equal to 1/5 of the amount she ordered?

Answer : The tip that Ashley wants to give amounts to \$15 x 1/5 = \$ << 15 * 1 / 5 = 3 >> 3 .

Hence , she will give a total of \$ 15 + \$ 3 = \$ << 15 + 3 = 18 >> 18 to the delivery man .

18

TriviaQA Factual Knowledge Example

Question : What is the second most common gas in the atmosphere?

Answer : Oxygen

wide-leaning deep-leaning

Figure 5: Token-level deep share for GSM8K and TriviaQA. Blue denotes wide-leaning (prefers the capacity path) while red denotes deep-leaning, meaning it prefers the compute (looped) path.

set $FLOP_{\text{ffn}}(d_{\text{ffn}}) = (\alpha(F_M - FLOP_{\text{gate}})/K) - FLOP_{\text{attn}}$ and analogously for the wide width with $(1 - \alpha)$. We then invert Eq. 8 for the *largest* d_{ffn} (rounded down to a multiple of 64) whose h_{eff} keeps the equation at or below the target – the “floor” rounding mode. The exception is PUREWIDE, where we round up (“ceil”); this keeps the largest single-axis capacity baseline honest by spending the entire budget and has strictly more FLOPs than the dual-path baselines. The residual mismatch is $< 2\%$ of F_M in every configuration.

C Model Configurations

All configurations share the same backbone: $L = 16$ layers, $d = 768$, $h_q = h_{kv} = 12$ (GQA repeat factor 1), sequence length 4096, vocabulary size 50,304, weight-tied input/output embeddings, and the SwiGLU effective-hidden rule of Appendix B (multiple of 64). Tables 2 and 3 list, for every model in this paper, the configured deep FFN width d_{ffn} , wide FFN width $d_{\text{ffn}}^{\text{wide}}$, recursion depth K , total parameter count, and wall-clock training time.

D Inference-time ablations

We probe the trained dual-path model ($F_M = 80\text{M}$, $\alpha = 50$, $K = 4$) at inference time, overriding either the loop count or the gate. Table 4 reports per-token cross-entropy on three Paloma sources.

The loop budget matters, and the schedule does not extrapolate. Forcing fewer loop iterations at inference monotonically degrades loss (e.g. GSM8K loss rises from 2.148 at the trained

$K=4$ to 3.592 at $K=1$). Returns diminish past the trained value, i.e. the loop dynamics learned at training do not extrapolate past the training budget.

Both paths are needed. Disabling either gate ($g_d=1, g_w=0$ or $g_d=0, g_w=1$) costs 3.6–5.6 nats across the three sources – larger than the gap between an early-training and a fully-trained model. A uniform 0.5:0.5 split still loses ~ 2.6 nats. Opening both gates fully ($g_d=1, g_w=1$) is the worst override: the model has trained with bounded gate magnitudes and the residual update is far out of its training distribution.

The per-token decision carries information. The shuffled-gates row keeps the marginal distribution of (g_d, g_w) but randomises which token gets which assignment within each sequence. Loss rises by 0.51–0.94 nats, indicating that the gate’s per-token decisions, not just its average behaviour are load-bearing.

E Evaluation Details

We evaluate language modelling on Paloma C4 and WikiText-103 (bits-per-byte). Commonsense is the mean over ARC-c, ARC-e, HellaSwag, PIQA, SIQA, and WinoGrande. Math is GSM8k accuracy and the OLMo3 base-easy math BPB average over Algebra, Counting, Geometry, Intermediate Algebra, Number Theory, Pre-algebra, and Pre-calculus. Note that for Figure 2 we average across BPB values from *all* benchmarks as listed in Table 5 ($F_M = 80\text{M}$) and Table 6 ($F_M = 160\text{M}$).

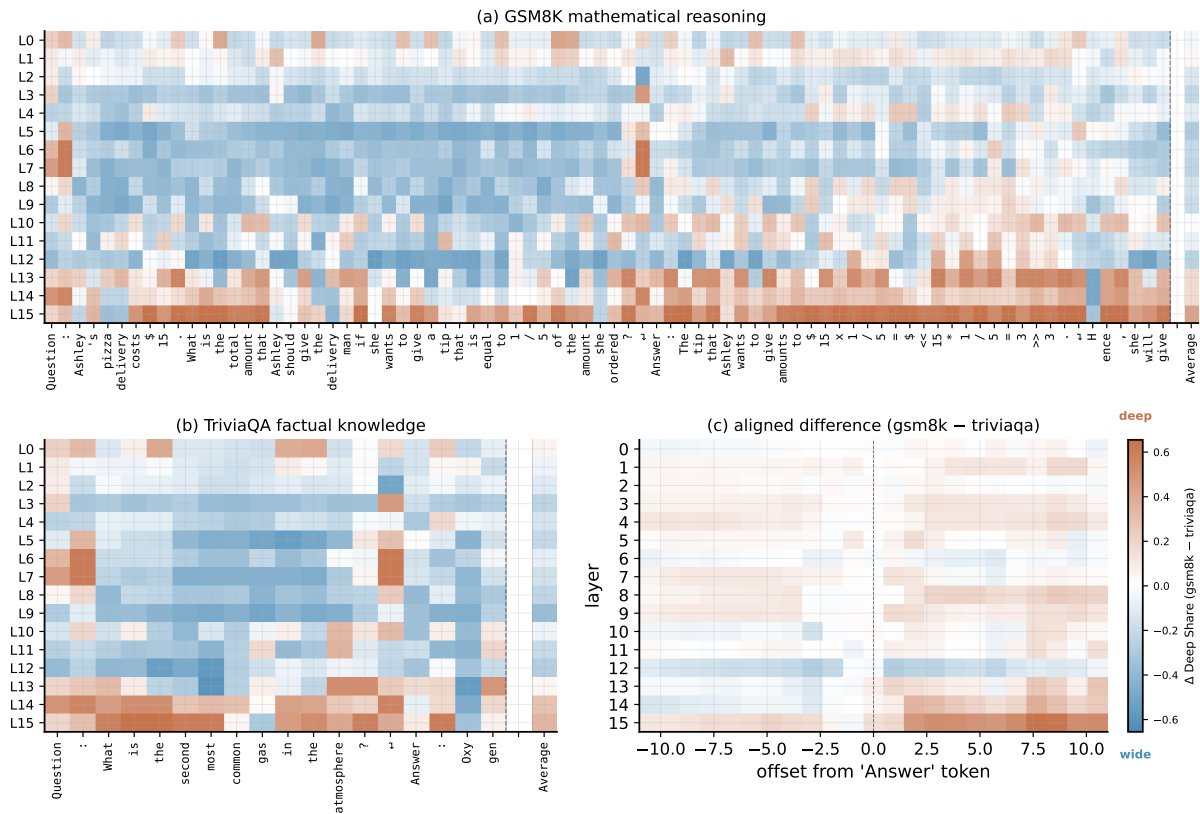


Figure 6: **Step-by-step token-level routing grid and task alignment.** Panel (a) shows the layer-by-token heatmap of the deep share for a sequence from GSM8K (mathematical reasoning). Panel (b) shows the heatmap for a sequence from TriviaQA (factual knowledge). Panel (c) shows the aligned difference in preference (gsm8k – triviaqa) around the anchor token “Answer”, averaged over one thousand sequences per dataset.

Evaluations are run using the OLMES evaluation framework (Gu et al., 2025).

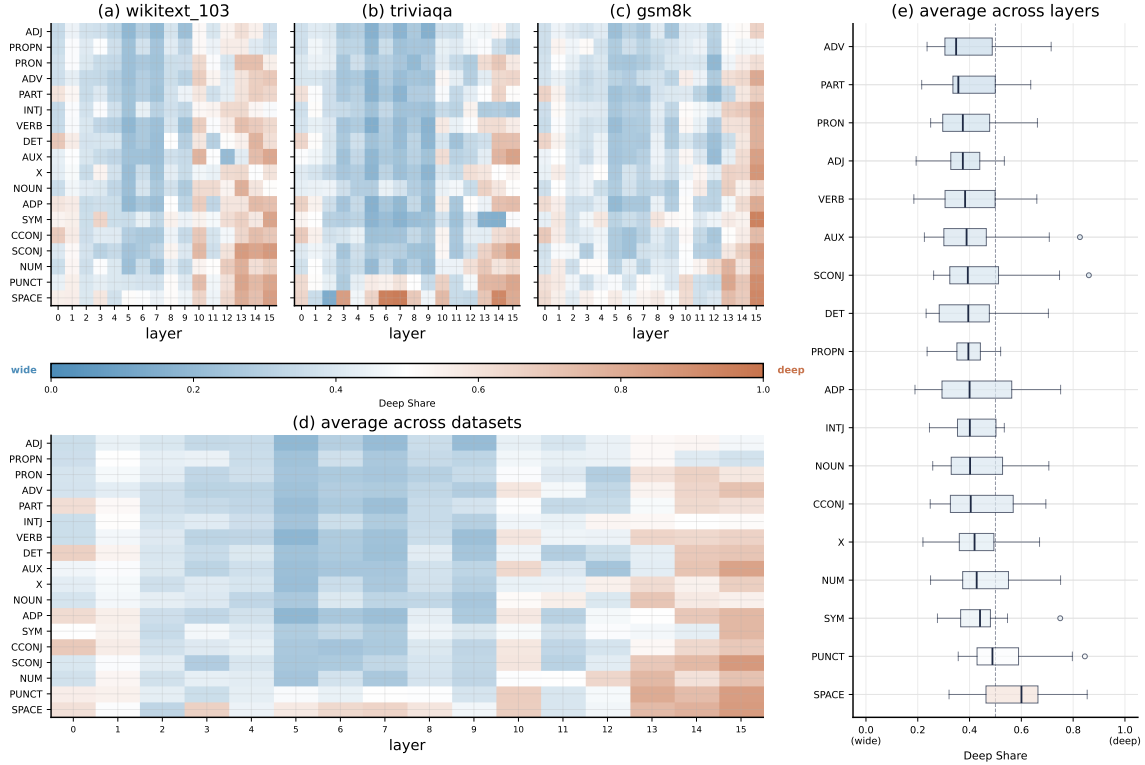


Figure 7: **Parts-of-speech (POS) routing characteristics and commitment.** Panels (a, b, c) show heatmaps of the mean deep share per universal POS tag across layers for `wikitext_103`, `triviaqa`, and `gsm8k`, respectively, with tags sorted by the overall mean deep share. Panel (d) plots the average heatmap across the three datasets. Panel (e) shows boxplots of the deep share distribution per POS tag across all layers and datasets, sorted by their median preference (most deep-leaning at the bottom).

Ablation	GSM8K	TriviaQA	WikiText-103
Learned router (baseline)	2.148	4.129	3.026
<i>Compute (force K loops; trained with K=4)</i>			
$K=1$	3.592 (+1.44)	5.777 (+1.65)	4.846 (+1.82)
$K=2$	2.665 (+0.52)	4.694 (+0.57)	3.842 (+0.82)
$K=3$	2.221 (+0.07)	4.174 (+0.05)	3.178 (+0.15)
$K=4$ (trained)	2.148 (+0.00)	4.129 (+0.00)	3.026 (+0.00)
$K=5$	2.206 (+0.06)	4.187 (+0.06)	3.046 (+0.02)
$K=6$	2.271 (+0.12)	4.239 (+0.11)	3.074 (+0.05)
$K=7$	2.323 (+0.18)	4.283 (+0.15)	3.098 (+0.07)
$K=8$	2.366 (+0.22)	4.320 (+0.19)	3.120 (+0.09)
$K=9$	2.405 (+0.26)	4.351 (+0.22)	3.140 (+0.11)
$K=10$	2.442 (+0.29)	4.380 (+0.25)	3.160 (+0.13)
<i>Gate overrides</i>			
$g_d=1, g_w=0$ (deep only)	7.684 (+5.54)	8.291 (+4.16)	8.090 (+5.06)
$g_d=0, g_w=1$ (wide only)	7.574 (+5.43)	7.747 (+3.62)	8.655 (+5.63)
$g_d=0.5, g_w=0.5$ (uniform)	4.744 (+2.60)	6.707 (+2.58)	5.749 (+2.72)
$g_d=1, g_w=1$ (fully open)	8.541 (+6.39)	9.099 (+4.97)	9.211 (+6.19)
Shuffled gates	2.658 (+0.51)	5.071 (+0.94)	3.720 (+0.69)

Table 4: Inference-time ablations of the dual-path router. We report per-token cross-entropy loss on three Paloma sources. **Compute (top block):** forcing exactly K loop iterations confirms that loop budget matters, with diminishing returns past the trained value. Extra inference loops beyond training degrade the model monotonically rather than plateauing, indicating the loop schedule does not extrapolate past its training budget. **Gate overrides (bottom block):** both paths are necessary, disabling either ($g_d=1, g_w=0$ or $g_d=0, g_w=1$) collapses performance.

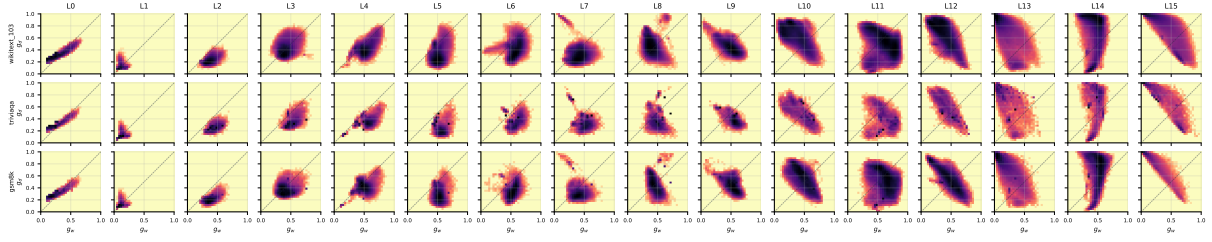


Figure 8: **Layer-wise joint density of raw gates** (g_w, g_d) across all layers ($L0$ to $L15$) and evaluation sources. The rows correspond to the three Paloma evaluation datasets (`wikitext_103`, `triviaqa`, and `gsm8k`), while columns correspond to layers index 0 to 15. The diagonal dashed line in each subplot represents equal routing preference ($g_d = g_w$). Lighter regions represent higher token concentration. The model has $L = 16$ layers, $K = 4$ loops, $d_{\text{model}} = 768$, deep FFN hidden width = 4864, wide FFN hidden width = 24448, dual $\alpha = 50$.

Table 5: Full results at the **F80M** FLOP budget. ℓ denotes the loop count. Commonsense Acc. / BPB are means over ARC-c, ARC-e, HellaSwag, PIQA, SIQA, WinoGrande. The OLMo3 easy math avg is the OLMo3 base-easy math BPB average. Best value in each row is **bold** (highest for accuracy \uparrow , lowest for BPB \downarrow).

Metric	PureWide	PureLoop ℓ_2	PureLoop ℓ_3	PureLoop ℓ_4	Dual-a25 ℓ_2	Dual-a50 ℓ_2	Dual-a75 ℓ_2	Dual-a25 ℓ_3	Dual-a50 ℓ_3	Dual-a75 ℓ_3	Dual-a25 ℓ_4	Dual-a50 ℓ_4	Dual-a75 ℓ_4
Params	719M	398M	294M	238M	644M	559M	483M	615M	511M	398M	606M	483M	360M
<i>Commonsense (avg)</i>													
Acc. \uparrow	0.5203	0.5036	0.5067	0.5031	0.5283	0.5265	0.5218	0.5239	0.5269	0.5192	0.5163	0.5256	0.5249
BPB \downarrow	0.9920	1.0028	1.0236	1.0352	0.9888	0.9826	0.9866	0.9827	0.9808	0.9870	0.9902	0.9820	0.9892
<i>Commonsense (per task, Acc. \uparrow / BPB \downarrow)</i>													
ARC-c Acc.	0.4053	0.3779	0.3770	0.3809	0.4307	0.4111	0.4346	0.4336	0.4004	0.3994	0.4014	0.4170	0.4072
ARC-c BPB	0.7967	0.8253	0.8546	0.8651	0.8001	0.7958	0.7954	0.7966	0.8016	0.8188	0.7974	0.7983	0.8090
ARC-e Acc.	0.7158	0.6953	0.6973	0.6875	0.7148	0.7305	0.7100	0.6973	0.7178	0.7119	0.7148	0.6982	0.7266
ARC-e BPB	0.5915	0.6134	0.6308	0.6801	0.5912	0.5779	0.5855	0.5907	0.5877	0.5820	0.5904	0.5912	0.6034
HellaSwag Acc.	0.3906	0.3730	0.3760	0.3643	0.4014	0.4131	0.4043	0.4121	0.4150	0.3965	0.3955	0.4150	0.3955
HellaSwag BPB	0.8947	0.8997	0.9156	0.9282	0.8872	0.8865	0.8928	0.8847	0.8888	0.8973	0.8940	0.8911	0.8946
PIQA Acc.	0.6475	0.6348	0.6436	0.6338	0.6533	0.6436	0.6455	0.6348	0.6582	0.6357	0.6289	0.6455	0.6367
PIQA BPB	1.1511	1.1816	1.1962	1.2069	1.1441	1.1524	1.1577	1.1504	1.1563	1.1646	1.1540	1.1627	1.1567
SIQA Acc.	0.4453	0.4346	0.4297	0.4326	0.4492	0.4346	0.4346	0.4385	0.4443	0.4453	0.4424	0.4424	0.4492
SIQA BPB	1.1863	1.2167	1.2252	1.2343	1.1983	1.2090	1.2101	1.1922	1.1625	1.1813	1.2147	1.1768	1.1975
WinoGrande Acc.	0.5176	0.5059	0.5166	0.5195	0.5205	0.5264	0.5202	0.5273	0.5254	0.5264	0.5146	0.5352	0.5342
WinoGrande BPB	1.3316	1.2803	1.3191	1.2964	1.3121	1.2741	1.2785	1.2819	1.2881	1.2782	1.2910	1.2716	1.2743
<i>Math</i>													
GSM8k Acc. \uparrow	0.0791	0.0723	0.0723	0.0527	0.0879	0.0801	0.1006	0.0879	0.1006	0.0820	0.0664	0.0898	0.0918
Algebra BPB \downarrow	0.5201	0.5306	0.5385	0.5468	0.5173	0.5162	0.5198	0.5178	0.5115	0.5186	0.5215	0.5173	0.5141
Counting BPB \downarrow	0.5240	0.5343	0.5479	0.5557	0.5228	0.5244	0.5289	0.5259	0.5232	0.5294	0.5289	0.5230	0.5252
Geometry BPB \downarrow	0.5622	0.5736	0.5860	0.6004	0.5571	0.5579	0.5667	0.5596	0.5568	0.5634	0.5579	0.5567	0.5605
Int. Algebra BPB \downarrow	0.5402	0.5538	0.5592	0.5707	0.5332	0.5281	0.5409	0.5358	0.5317	0.5377	0.5372	0.5262	0.5334
Number Theory BPB \downarrow	0.5940	0.6057	0.6137	0.6218	0.5926	0.5902	0.5937	0.5924	0.5892	0.5981	0.5950	0.5870	0.5885
Pre-algebra BPB \downarrow	0.5069	0.5155	0.5237	0.5322	0.5061	0.5033	0.5087	0.5051	0.5005	0.5078	0.5095	0.5036	0.5048
Pre-calculus BPB \downarrow	0.4357	0.4470	0.4488	0.4670	0.4306	0.4252	0.4391	0.4316	0.4315	0.4335	0.4272	0.4247	0.4325
Easy math avg BPB \downarrow	0.5261	0.5372	0.5454	0.5564	0.5228	0.5208	0.5282	0.5240	0.5206	0.5269	0.5253	0.5198	0.5227
<i>Reading / QA</i>													
LAMBADA Acc. \uparrow	0.2861	0.2803	0.2744	0.2793	0.2949	0.2725	0.2939	0.2832	0.3135	0.2881	0.2988	0.3037	0.3076
LAMBADA BPB \downarrow	0.9492	0.9769	0.9887	1.0032	0.9161	0.9454	0.9342	0.9167	0.9146	0.9462	0.9341	0.9154	0.9473
QASPER Acc. \uparrow	0.5987	0.6740	0.6771	0.6771	0.6646	0.5361	0.6677	0.6301	0.5862	0.6803	0.6301	0.4765	0.6771
QASPER BPB \downarrow	0.3063	0.3098	0.3150	0.3233	0.3012	0.3030	0.3010	0.3035	0.3027	0.3020	0.2992	0.3108	0.3081
<i>Paloma (BPB \downarrow)</i>													
C4	1.0370	1.0513	1.0652	1.0777	1.0311	1.0374	1.0395	1.0331	1.0358	1.0472	1.0374	1.0362	1.0451
WikiText-103	0.9461	0.9608	0.9757	0.9918	0.9373	0.9453	0.9477	0.9344	0.9382	0.9508	0.9420	0.9393	0.9480

Table 6: Full results at the **F160M** FLOP budget. ℓ denotes the loop count. Commonsense Acc. / BPB are means over ARC-c, ARC-e, HellaSwag, PIQA, SIQA, WinoGrande. The OLMo3 easy math avg is the OLMo3 base-easy math BPB average. Best value in each row is **bold** (highest for accuracy \uparrow , lowest for BPB \downarrow).

Metric	PureWide	PureLoop ℓ_2	PureLoop ℓ_3	PureLoop ℓ_4	Dual-a25 ℓ_2	Dual-a50 ℓ_2	Dual-a75 ℓ_2	Dual-a25 ℓ_3	Dual-a50 ℓ_3	Dual-a75 ℓ_3	Dual-a25 ℓ_4	Dual-a50 ℓ_4	Dual-a75 ℓ_4
Params	1361M	719M	502M	398M	1200M	1040M	880M	1153M	936M	719M	1125M	880M	644M
<i>Commonsense (avg)</i>													
Acc. \uparrow	0.5384	0.5303	0.5244	0.5137	0.5374	0.5358	0.5202	0.5493	0.5360	0.5384	0.5420	0.5326	0.5335
BPB \downarrow	0.9636	0.9814	0.9894	1.0010	0.9755	0.9608	0.9744	0.9655	0.9572	0.9572	0.9610	0.9704	0.9700
<i>Commonsense (per task, Acc. \uparrow / BPB \downarrow)</i>													
ARC-c Acc.	0.4277	0.4170	0.4053	0.3896	0.4365	0.4160	0.4150	0.4346	0.4326	0.4316	0.4482	0.4512	0.4375
ARC-c BPB	0.7715	0.7880	0.8107	0.8178	0.7758	0.7674	0.7746	0.7839	0.7652	0.7704	0.7800	0.7673	0.7730
ARC-e Acc.	0.7520	0.7266	0.7109	0.7051	0.7207	0.7275	0.7129	0.7461	0.7305	0.7314	0.7373	0.7324	0.7363
ARC-e BPB	0.5558	0.5717	0.5961	0.6046	0.5634	0.5579	0.5682	0.5610	0.5633	0.5606	0.5624	0.5775	0.5668
HellaSwag Acc.	0.4229	0.4248	0.4004	0.4043	0.4414	0.4316	0.4111	0.4404	0.4258	0.4219	0.4277	0.4209	0.4170
HellaSwag BPB	0.8767	0.8809	0.8935	0.8929	0.8670	0.8723	0.8827	0.8696	0.8705	0.8738	0.8661	0.8796	0.8759
PIQA Acc.	0.6689	0.6445	0.6455	0.6367	0.6777	0.6592	0.6436	0.6660	0.6543	0.6611	0.6494	0.6602	0.6562
PIQA BPB	1.1263	1.1494	1.1660	1.1705	1.1145	1.1259	1.1336	1.1181	1.1185	1.1304	1.1367	1.1354	1.1349
SIQA Acc.	0.4541	0.4463	0.4414	0.4395	0.4395	0.4541	0.4463	0.4658	0.4434	0.4492	0.4502	0.4277	0.4443
SIQA BPB	1.1906	1.2077	1.2048	1.2272	1.1524	1.1695	1.1809	1.1780	1.1751	1.1639	1.1638	1.1794	1.1893
WinoGrande Acc.	0.5049	0.5225	0.5430	0.5068	0.5088	0.5264	0.4922	0.5430	0.5293	0.5352	0.5391	0.5029	0.5098
WinoGrande BPB	1.2609	1.2908	1.2650	1.2932	1.3800	1.2719	1.3063	1.2826	1.2509	1.2439	1.2572	1.2830	1.2802
<i>Math</i>													
GSM8k Acc. \uparrow	0.1250	0.1045	0.1191	0.0938	0.0996	0.1084	0.1055	0.1084	0.1074	0.1094	0.1250	0.1328	0.1406
Algebra BPB \downarrow	0.5038	0.5013	0.5101	0.5114	0.5074	0.5081	0.5049	0.5043	0.5007	0.5041	0.5018	0.4920	0.4976
Counting BPB \downarrow	0.5115	0.5112	0.5200	0.5242	0.5127	0.5147	0.5157	0.5135	0.5098	0.5129	0.5129	0.5031	0.5083
Geometry BPB \downarrow	0.5419	0.5426	0.5466	0.5585	0.5397	0.5457	0.5478	0.5383	0.5389	0.5440	0.5369	0.5282	0.5404
Int. Algebra BPB \downarrow	0.5137	0.5201	0.5250	0.5282	0.5208	0.5215	0.5243	0.5175	0.5186	0.5191	0.5154	0.5003	0.5145
Number Theory BPB \downarrow	0.5751	0.5783	0.5840	0.5872	0.5804	0.5840	0.5784	0.5804	0.5769	0.5758	0.5758	0.5632	0.5699
Pre-algebra BPB \downarrow	0.4923	0.4924	0.4974	0.5007	0.4942	0.4964	0.4956	0.4920	0.4913	0.4928	0.4917	0.4831	0.4864
Pre-calculus BPB \downarrow	0.4154	0.4177	0.4221	0.4289	0.4210	0.4231	0.4239	0.4135	0.4137	0.4165	0.4117	0.4010	0.4155
Easy math avg BPB \downarrow	0.5077	0.5091	0.5150	0.5199	0.5109	0.5134	0.5130	0.5085	0.5071	0.5093	0.5066	0.4959	0.5047
<i>Reading / QA</i>													
LAMBADA Acc. \uparrow	0.3086	0.3135	0.2920	0.2939	0.3115	0.2979	0.2822	0.2959	0.3115	0.3223	0.3105	0.3271	0.3203
LAMBADA BPB \downarrow	0.9169	0.9038	0.9408	0.9359	0.8811	0.8997	0.9184	0.9031	0.8985	0.8780	0.8854	0.8646	0.8945
QASPER Acc. \uparrow	0.5768	0.6301	0.6583	0.5987	0.6583	0.6207	0.6803	0.6865	0.5799	0.6301	0.4514	0.5925	0.6050
QASPER BPB \downarrow	0.2964	0.2990	0.2916	0.2941	0.3120	0.3405	0.2982	0.3112	0.3215	0.2963	0.3247	0.3309	0.2934
<i>Paloma (BPB \downarrow)</i>													
C4	1.0183	1.0270	1.0367	1.0446	1.0130	1.0163	1.0203	1.0138	1.0138	1.0188	1.0129	1.0166	1.0212
WikiText-103	0.9224	0.9312	0.9388	0.9453	0.9137	0.9208	0.9220	0.9177	0.9147	0.9214	0.9108	0.9201	0.9241